Proceedings of the
International Conference on Mechanical Engineering 2009
(ICME2009) 26- 28 December 2009, Dhaka, Bangladesh

ICME09-RT-50

THE DEVELOPMENT OF A COMPUTER VISION BASED REAL-TIME INSPECTION SYSTEM TO DETECT THE STATUS OF AUTOMOBILE BREAK TUBE

S. Ahasan Ahammad[1], E. Naranbaatar[2] and B. Ryong Lee[3]

[1]Graduate School of Institute of e-vehicle Technology, University of Ulsan, Ulsan, Korea
[2]Department of Mechanical & Automotive Engineering, University of Ulsan, Ulsan, Korea
[3]School of Mechanical & Automotive Engineering, University of Ulsan, Ulsan, Korea

ABSTRACT

Getting high quality products with a rapid and accurate inspection system is the most important aspect in manufacturing field. It is almost impossible to check the fault of all parts coming from part-feeding system, with only human inspection because of time limitation and working hardship as well. Therefore, most of the manual inspections which are applied to specific samples instead of all coming parts can neither guarantee consistent measuring accuracy nor decrease working time. In order to improve the measuring speed and accuracy of the inspection, a computer-aided measuring and analysis method is highly required. In this paper, a computer-vision-based automobile brake tube inspection algorithm is proposed, where a modified Hough transform is applied for calculating the geometry of straight line segments and a line-scanning method is adopted to compute the center points of the inner and outer diameters. Finally, the proposed algorithms are verified by the developed inspection machine to fulfill the inspection requirements demanded from the company.

Keywords: Edge Detection, Hough Transform, Computer Vision, Forming-Error Inspection.

1. INTRODUCTION

Computer vision systems, as part of factory automation systems, could be used for quality inspection, classification, recognition, etc., instead of human vision [1, 2].

Recently, factory automation technology in manufacturing has been growing rapidly. However, the inspection process, which is the last step of manufacturing, remains at a minimal level of technology. Most part inspection processes still depend on human vision. Conventional human vision-based inspection causes problems such as eye exhaustion, concentration decreases, inconsistent criterion, difficulty in fast feedback, and high labor costs, etc. One alternative method is to apply a computer vision system to the factory automation. Since the mid-1980's, vision inspection systems using CCD cameras have been studied and proven to have advantages of low cost and system simplicity. Exact predictions of the performances of the Hough detection of straight lines in two-dimensional images are presented for rectangular and circular retinas, in Cartesian and normal parameterization [3], in the case of noisy signals, image processing for industrial applications has been studied in Europe [4], vision inspection systems for IC chip fault detection have been studied, in which custom integrated circuits make it possible to realize four basic operations in a compact way: shape recognition, mask generation, programmable image delay, and subsample filtering [5]. An example that has been processed by a hardware realization of such a pipeline system is provided. Toshiyuki et al. [6] developed an algorithm for a book sorting system using pattern matching. Shapiro et al. [7] developed a failure inspection system for ALC blocks which improved measurement resolution from 0.05 cm to 0.01 cm. As stated above, an inspection system using CCD cameras needs to draw out the feature of the edge for specific parts. The Hough transform among the feature detection methods has been developed to analytically detect definable shapes (line, circle, ellipse etc.) from image data. The main advantage of the Hough transform is achieving robustness against noise; however, one disadvantage if the method is that it requires a large memory and preliminary information of the shape for an exact partition [8-10]. In the matching tasks which form an integral part of all types of tracking and geometrical vision, there are invariably priors available on the absolute and/or relative image locations of features of interest. Usually, these priors are used post-hoc in the process of resolving feature matches and obtaining final scene estimates via 'first get candidate matches, then resolve' consensus algorithms such as RANSAC [11].

In this paper, a computer vision-based inspection

system was developed to inspect the forming status of brake tubes used for automobiles. The system discriminates whether the formed part of the tube is normal or abnormal in both shape and dimension. The inspection algorithm detects line segments from a side-view image using a Hough transform; it finds the slope angle of the formed area, eccentricity and diameters of the tube. Using a front-view image, the center points of the inner and outer diameters are calculated to determine the abnormity of the tubes by applying a line-scanning method.

2. TUBE FAULT DETECTION ALGORITHMS

As explained before, tubes considered in this paper were formed at their end point. The formed shape is important to secure the safety in the brake line. If the formed shape is abnormal and combined loosely to the counterpart, there may be high risk in powerful braking because of oil leakage. As a result, it is important to correctly inspect the status of the formed shape to reduce the potential risk of the vehicle. The side-view image of the formed shape of the tube is shown in Fig. 1.

Fig 1. Exemplary side-view image of the formed tube

In this section, a new forming error detection algorithm for a brake tube is proposed. The overall algorithm consists of three main kinds of sub-algorithms: front-view, side-view and threaded nut inspection algorithms. The front-view inspection sub-algorithm calculates inner and outer diameters using a line scanning method. The side-view inspection algorithm extracts line segments of the formed tube-end and calculates the slope angles of the tube-end using a Hough transform technique. From the slope angles, the eccentricity information of the formed area can be acquired. Then, by checking the eccentricity, we can classify the part as either normal or abnormal. The full flowchart of the forming error inspection procedure of the system is shown in Fig. 2.

2.1 Side-View Inspection Algorithm

For the side-view inspection, a Hough transform is adopted. Considering line $y = ax + b$, parameters a and b can have values in the range of $-\infty<a<\infty$ and $-\infty<b<\infty$. Therefore, it is difficult to express the line equation in the parametric space, and a lot of memory quantity is needed to store each line data. If the line $y = ax + b$ is represented as $\rho = x\cos\theta + y\sin\theta$ then the range of ρ and θ can be limited between $-N\sqrt{2} \le \rho \le N\sqrt{2}$ and $-\pi \le \theta \le \pi$, respectively. The quantity of memory and calculation difficulties can be efficiently reduced because of the limited range of the parameters. However, some additional treatment should be considered to further reduce the inspection time. For this purpose, we used a clustering structure in which a subset area with relatively many points is found.

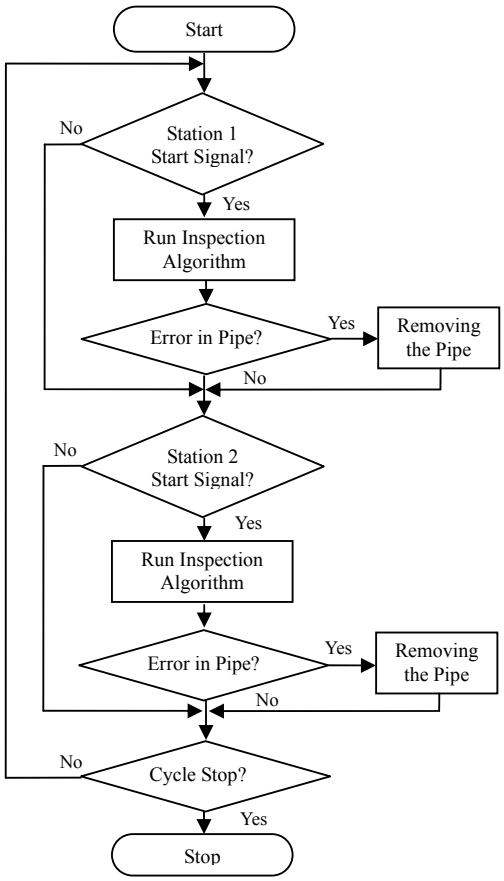

Fig 2. Overall flowchart of tube-fault-detection

The straight line equation obtained from a set of partial points may have some fuzzy distribution because of the noise effect of the Hough transform [13]. Therefore, the line equation needed to be approximated using the Gaussian function [14]. Its center point was calculated with the average of the points belonging to the cluster. Through the side-view inspection, tube type was identified by calculating the diameter of the tube stem. Slope angle of the formed conical shape was also calculated, from which the important eccentricity information was calculated. To classify the tube type, we averaged the diameters given from some sampled diameters as shown in Fig. 3. The average diameter of the tube can be calculated using the Eq. (1).

$$D_{average} = \frac{1}{n}\sum_{i=1}^{n}(P_{ri} - P_{li}) \qquad (1)$$

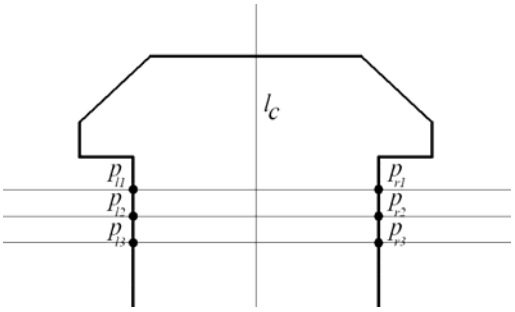

Fig 3. Schematic diagram of diameter calculation using sampled scan data

The inclined lines are determined in the slope surface using Hough transform. Due to noise, in accumulator space, there are several higher voted values (lines) neighboring the real line which is shown in Fig. 4. The accumulator space's highest voted value is used to determine the inclined line which some time does not represent the real line due to noise like sticky scraps on the inclined surface made from forming process. To solve this difficulty, we consider four highest values form the accumulator space and average these values to get the more reliable result. The average parameterized line equation can be calculated using the Eq. (2).

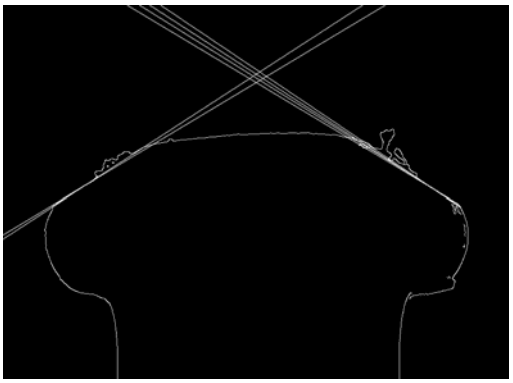

Fig 4. Over lapped inclined lines on slope detection

$$\rho = \frac{1}{n}\sum_{i=1}^{n}\left(x \cdot Cos\theta_n + y \cdot Sin\theta_n\right) \qquad (2)$$

where ρ is the distance between the line and the origin and θ is the angle of the vector from the origin to this closest point.

Once the tube type was identified, the slope angle of the formed area and eccentricity could be calculated using the geometric relations, as shown in Fig. 5.

In Fig. 5, the slope angle of the formed tube, denoted as γ, can be calculated by the Eq. (3).

$$\begin{aligned} \gamma_1 &= \alpha \\ \gamma_2 &= 180^o - \beta \\ \gamma &= \gamma_1 + \gamma_2 \end{aligned} \qquad (3)$$

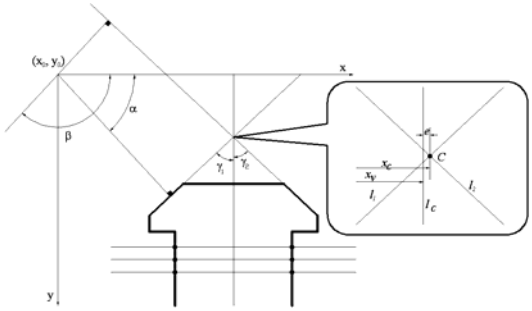

Fig 5. Schematic diagram for finding eccentricity using slope angles and center line of the tube stem

In fact, the slope angle is an important parameter for checking whether the formed tube is normal or not. Another important parameter for the normality test is eccentricity. In Fig. 5, l_1 and l_2 describe the inclined lines representing the slope surfaces of the tube. The intersection point of the two lines is denoted as point C. When a line l_c is defined as the line bisecting the tube stem, the eccentricity e is defined as the off-set displacement from l_c to the intersection point C by the Eq. (4).

$$e = | x_c - x_v | \qquad (4)$$

where x_c and x_v is the x coordinate value of point C and line l_c respectively.

Eccentricity is a critical criterion for the normality test. However, it was not easy to calculate the slope angles precisely because of noise on the inclined line due to light reflection. Therefore we adopted the Hough transform to find the correct line information on the lines, even in the presence of considerable noise.

In general, a Hough transform requires abundant memory and time because it considers the whole angular space in the image plane. In our case, we can obtain some pre-determined shape information from the tube. Hence, we can confine the angular space in the image. Since the slope angle of the lines for the normal pipe is known to be ±28°, the search range of the slope angle can be divided by ten: 0.5° interval from +26° to +31°, likewise a 0.5° interval from -26° to -31°. Hence, a total of 20 parametric spaces were selected for the Hough transform.

2.2 Front-View Inspection Algorithm

In the front-view inspection, we calculate the inner diameter and outer diameter as well as the center point of the front image. H. S. Kim and B. R. Lee [15, 16] proposed a line scanning method which scans the front image of the tube in both horizontal and vertical directions inside a specific region. However, when there is an impure material or a lump of dust inside the tube, the method may give the wrong geometric information for the tube. To avoid this weakness, we applied a radial scanning method to measure the radius of the inner circle

of the tube. An exemplary tube image describing the scanning method is shown in Fig. 6.

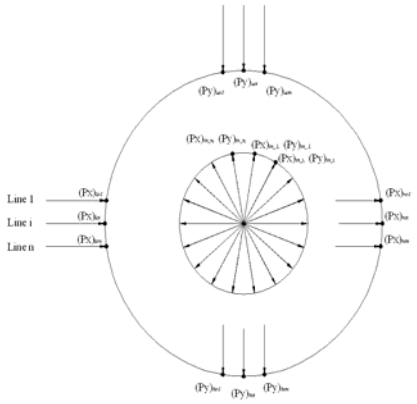

Fig 6. Scanning methods to find the center and radius

Using a number of scanning lines along both x and y directions, the x- and y-coordinate values of the tube center can be calculated. Fig. 5 shows how to find the x-coordinate value of the circle center. Center position and radius are averaged among their values from the scanning lines to increase measuring accuracy. The radius of the outer circle and the coordinate of the center position can be calculated by the Eqs. (5) ~ (7).

$$R_o = \frac{1}{2n}\sum_{i=1}^{n}\left[(P_x)_{roi} - (P_x)_{loi}\right] \quad (5)$$

$$X_{center} = \frac{1}{n}\sum_{i=1}^{n}\left[\frac{(P_x)_{loi} + (P_x)_{roi}}{2}\right] \quad (6)$$

$$Y_{center} = \frac{1}{n}\sum_{i=1}^{n}\left[\frac{(P_y)_{uoi} + (P_y)_{boi}}{2}\right] \quad (7)$$

When the center position of the circle is known, we can calculate the radius of the inner circle by considering the length between the center position of the circle and points on the circle. Thus, the average radius of the inner circle can be calculated by using Eq. (8).

$$R_i = \left(\sum_{i=1}^{n}\sqrt{((P_x)_{in\_i} - X_{center})^2 + ((P_y)_{in\_i} - Y_{center})^2}\right)/n \quad (8)$$

where P is a point on the inner circle.

3. EXPERIMENTAL SETUP AND PIPE-FAULT-DETECTION

To inspect the forming status at both ends of the formed tubes, we implemented computer vision-based experimental equipment. For this purpose, three CCD cameras were used at each end of the tube. Cameras (Sony, model XC-HR70) were used to inspect front-view, side-view and nut-view. The lenses used were TCL 04S-3 for front-view, TCL 04L-3 for side-view, and ML-2514 for nut-view. A Matrox II frame grabber was used to capture images and transfer them to the computer. The Mil-Lite library was used for communication between Microsoft Visual C++ 6.0 and the Matrox II frame grabber. Open CV Library was used for basic operations such as filtering, feature detection, etc. A clamp and a stopper were operated by an air cylinder to make a position and hold the formed tube at the test bed while the vision inspection process was running. Master K80S PLC was used to control the clamp and stopper, and to receive the inspection-end signal from the computer. The photograph of the implemented computer vision-based inspection system is shown in Fig. 7.

Fig 7. Implemented computer vision-based inspection system

To inspect with good accuracy, we need to secure the pipe and capture the image. To secure the pipe, we used a stopper and clamp. First, the pipe needs to be pushed until it touches the stopper, and then the clamp comes down to fix the pipe in place. After this, the stopper needs to return to its initial position; otherwise it will cover the front view inspection area.

Using the images taken from the front- and side-view profiles and the proposed algorithm, the outer diameter, inner diameter, slope angle, and eccentricity were calculated, and the pipe was determined to be normal or faulty. Table 1 shows the criteria usually used in the tube manufacturing company to determine whether the tested tube is normal or abnormal. To apply the standards in Table 1, a real length per unit pixel had to be found. In this paper, the length per unit pixel was set up as 0.001 mm/pixel based on real experiments, which fitting real measurement as mm in inspection measurement as pixel. In the experiment, image distortion compensation was not considered because the focal length of the lens was too short, distance is constant between camera and object and the view size was very small, at 5x5 mm^2, which does not cause big differences between distorted and undistorted images.

Table 1: Parameter criteria for normally formed tubes

Criterion			
Outer Diameter (mm)	Inner Diameter (mm)	Angle (°)	Eccentricity (mm)
7.1±0.18	3.2±0.13	114.5±0.5	0±0.1

3.1 Inspection Test for Normal Tube

For the inspection test, normal and abnormal tubes were prepared and the proposed inspection algorithm was tested to prove its feasibility. Fig. 8 shows a processed front-view image after edge detection and radius detection algorithms were applied. The four small circles found on the outer circle represent the core points for left, right, top, and bottom ends which were needed to calculate the radius of the outer circle and its center point based on the line scanning method. Once the center point was known, the radius of the inner circle was calculated by averaging the radial lines between the center point and the inner circle, which were generated by the radial scanning method. The outer and inner diameters were calculated to be 7.078 mm and 3.195 mm, respectively, using Eqs. (5) to (8). The measured dimensions for the inner and outer circles were in the range of the allowance designated in Table 1.

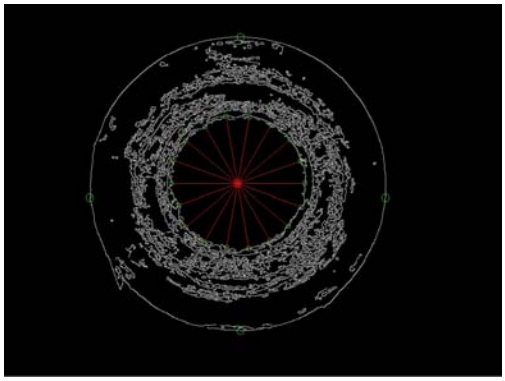

Fig 8. Processed front-view image for a normal tube

Figure 9 shows a processed side-view image after some preprocessing such as edge detection, line scanning, and a Hough transform to draw two inclined lines representing the formed surface of the tube. The lower three thin horizontal lines represent scanning lines for detecting the center line of the tube stem. A reference point was considered in the image. The reference point was decided as an intersection point of a horizontal line passing through the upmost brightest pixels and center line of the tube. All windows for region-of-interests were calculated as relative distances to the reference point. This way, all windows could trace the regions-of-interest even if the tube was placed in a slightly different position than the position preset. The four small squares (upper two and lower two) were regions of interest to find the thickness of the formed area of the tube. The two larger rectangles were regions to calculate the inclined lines of the formed area. The calculated slope angle of the formed area, defined as γ in Eq. (3), was 114.8 degrees. The eccentricity, defined as the off-set displacement from the coaxial line of the tube to the intersection point of the two inclined lines, was calculated as 0.058 mm. The measured two parameters were in the range of the allowable tolerance designated in Table 1.

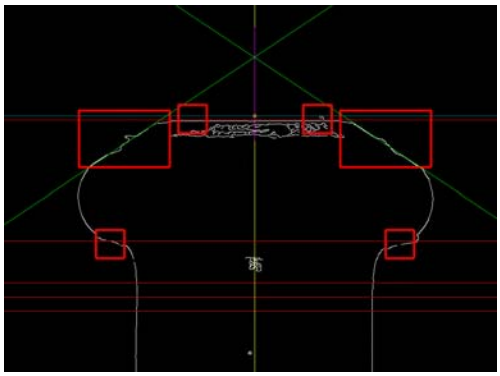

Fig 9. Processed side-view image for a normal tube

3.2 Inspection Test for Abnormal Tube

Figure 10 shows the processed image for a front-view inspection for a given abnormal tube, where the dimensions of the inner and outer diameters were 3.158 mm and 7.102 mm, respectively, which satisfies the allowable tolerance for normality regarding inner and outer diameters. However, it is necessary to check the eccentricity of the formed head to prove whether the tube is normal in all parameters.

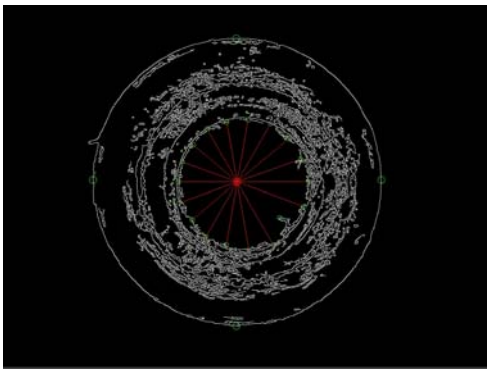

Fig 10. Processed front-view image for an abnormal tube

Figure 11 shows the image of a side-view inspection. As shown in the figure, the eccentricity was relatively big, which means that the tube has a large distance between the intersection point of the slope and center line because

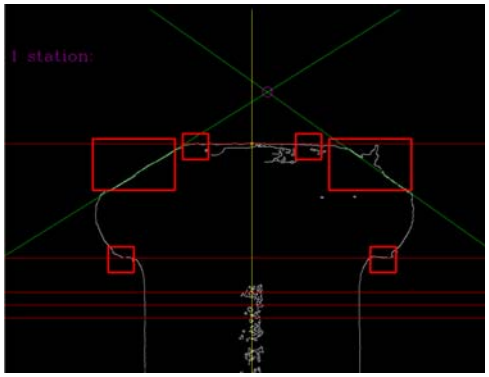

Fig 11. Processed side-view image for an abnormal tube

of a forming fault. The measured eccentricity and the slope angle are 0.348 mm and 112.9 degrees, respectively. According to the front-view and side-view inspections, the forming status of the tube was not normal.

3.3 Repeatability and Accuracy Tests

Two kinds of performance tests, repeatability and accuracy, were carried out. In the repeatability test, iterative measurements were performed on the same tube to show the robustness of the measurement. In the accuracy test, dimensions of the measured parts from the proposed vision inspection were compared to those of a 3-D measurement system. Table 2 shows results of the repeatability test, where five parameters of the tube were measured 10 times. As shown in Table 2, the test results were good; there exists no deviations in the outer diameter or angle. Only a 0.01 level of deviation was observed for the inner diameter, thickness, and eccentricity. This level of deviation is below the allowable deviation for most manufacturing lines.

Table 2 Repeatability test results for a sample tube

No	Outer diameter	Inner diameter	Angle	Thickness	Eccentricity
1	7.13	3.21	114.4	2.47	0
2	7.13	3.21	114.4	2.48	0
3	7.13	3.21	114.4	2.48	0
4	7.13	3.20	114.4	2.47	0
5	7.13	3.21	114.4	2.47	0
6	7.13	3.21	114.4	2.48	0.012
7	7.13	3.20	114.4	2.47	0
8	7.13	3.21	114.4	2.47	0
9	7.13	3.21	114.4	2.47	0
10	7.13	3.21	114.4	2.47	0

4. CONCLUSION

In this paper, we developed a vision-based fault inspection system and algorithm that can inspect all pipes coming from the forging machine. The system determines whether the pipe is normal or abnormal and the faulty pipe is discarded by a removing actuator. At the same time, the inspection result data and image files are delivered to the server computer. A modified Hough transform and line scanning method are used to analyze the pre-processed image, and the status of the pipe is determined to be satisfactory or defective.

The forging machine takes about 1 sec to draw the pipe, form and release the pipe. That means the whole inspection time could be accomplished in a second. The inspection system spends about 720 milliseconds (ms) to complete the inspection process, including the signaling time from/to the main controller. Therefore, the developed inspection system satisfies the required time. Also, data overflow problems with stacks of data and image files are solved.

In general, the pipes produced in the plant have 0.04 mm of eccentricity. Sometimes this may cause a problem for determining fault status. Since the inspection system can guarantee an accuracy of 0.01 mm, it can remove the decision error from pipe irregularity. Therefore, it is concluded that the developed inspection can be successfully applied to a real plant system to satisfy all the requirements.

5. REFERENCES

1. Otsu, N., 1979, "A Threshold Selection Method from Gray-Level Histograms", IEEE Trans. Syst. Man Cybernet, SMC-9, pp. 62-66.
2. Park, H. J., Hwan, Y. M., 2001, "*Dimensional Measurement Using the Machine Vision*", KSPE, Vol. 18, NO.3, pp. 10-17.
3. Maitre, H., 1986, "Contribution to the Prediction of Prediction of Performance of the Hough Transform", IEEE Trans. on Patten Analysis and Machine Intelligence, PAMI-8.5.
4. Braggins, D. W., 1990, "Image Processing for Industrial Applications in Europe", *Proc. 5th International Conference on Robot Vision and Sensory Control*, pp. 13-23.
5. Persoon, E., 1988, "A Pipelined Analysis System Using Custom Integrated Circuits", IEEE On Patten Analysis and Machine Intelligence, Vol. 10. No.1, pp. 110-116.
6. Gotoh, T., Toriu, T., Sasaki, S., 1988, "A Flexible Vision-Based Algorithm for a Book Sorting System", IEEE On Patten Analysis and Machine Intelligence, Vol. 10, No. 3, pp. 393-399.
7. Shapiro, S. D., 1975, "Transform for the Computer Detection of Curves in Noisy Picture", Comp. Graphics Image Process. 4, pp. 328-338.
8. Ballad, D. H., 1981, "Generalizing the Hough Transform to Detect Arbitrary Shapes", Pattern Recognition, 13, pp. 111-121.
9. Leavers, V. F., 1990, "The Dynamic Generalized Hough Transform", 1st *European Conference on Computer Vision (ECCV 1990),* Antibes, France.
10. Califano, A., Tayler, R. W., 1989, "A New Approach to Complex Parameter Feature Extraction", IEEE on Patten Analysis and Machine Intelligence, pp. 192-199.
11. Margarita Chli and Andrew J. Davison., 2008, "Active Matching", *10th European Conference on Computer Vision (ECCV 2008),* Antibes, France.
12. P.GU., 1994, "A Knowledge-Based Inspection Process Planning System for Coordinate Measuring Machines", Journal of Intelligent Manufacturing, pp. 351-363.
13. Etienne E. Kerre and Mike Nachtegael, 2000, Fuzzy Techniques in Image Processing, pp. 222-246.
14. R. Hartley and A. Zisserman, 2003, Multiple View Geometry in Computer Vision, Cambridge University Press, Second Edition, pp. 102-104.
15. H. S. Kim and B. R. Lee, 2006, "Real-Time Pipe Fault Detection System Using Computer Vision", International Journal of Precision Engineering and Manufacturing, Vol. 7, No. 1, pp. 30-34.
16. H. S. Kim, E. Naranbaatar, Sheikh Ahasan Ahammad, Y. H. Bae and B. R. Lee, 2009, "Real-Time Forming Error Inspection System using Computer Vision for Small-Sized Tubes", ICROS -SICE 2009, Fukuoka, Japan, pp 1950-19554.